

Hazard evaluation with closed pressure vessel test

Yusaku Iwata*[†]

*National Research Institute of Fire and Disaster, 4-35-3 Jindaijihigashi-machi Chofu Tokyo 182-8508, JAPAN

Phone : +81-422-44-8441

[†]Corresponding author : iwata@fri.go.jp

Received : August 28, 2015 Accepted : January 5, 2016

Abstract

A closed pressure vessel test (CPVT) was developed in order to measure the temperature and the pressure in the decomposition of sample. It is easier to measure the data with the CPVT than high sensitive calorimeters. The examples of sample were linseed oil, bio diesel fuel, refuse derived fuel, coal, a lithium coin battery and a lithium ion battery.

The results of CPVT measurements were compared with the results measured with a high sensitivity calorimeter (C80) and a spontaneous ignition tester (SIT), and a differential accelerating rate calorimeter (DARC). The data without the heat capacity correction for the sample vessel (ϕ correction) can be directly obtained with the DARC. The hazard of the oxidation heat and the intensity of decomposition in heating were investigated with the CPVT, the C80, the SIT and the DARC.

Keywords : auto-ignition, high sensitive calorimeter, spontaneous ignition tester, differential accelerating rate calorimeter

1. Introduction

There is the possibility that the oxidation heat causes a fire. It is useful for prevention of the fire to examine the hazard of the oxidation heat. The high sensitive calorimeter has been commonly used to investigate the oxidation heat because the oxidation heat is small. A closed pressure vessel test (CPVT) is developed in order to measure the oxidation heat easier than the high sensitive calorimeter. The sample of the gram order is used in the CPVT to detect the heat oxidation. The temperature and pressure in the decomposition of sample are measured with the CPVT. The data obtained with the CPVT are useful for the fire hazard evaluation of the sample which generates the oxidation heat. The measurement results of the CPVT are compared with those of a high sensitivity calorimeter (C80) and a spontaneous ignition tester (SIT) because there are few data of CPVT. The heat detection temperature are chosen as the hazard index of the auto-ignition by oxidation. Bio diesel fuel (BDF), linseed oil, squalane, and squalene are measured as liquid samples. Refuse derived fuel (RDF), refuse paper and plastic fuel (RPF) and subbituminous coal are measured as solid samples. It is an important point whether the generation of small heat by oxidation can be measured with the CPVT.

On the other hand, it is difficult to measure the intensity

of decomposition with the high sensitive calorimeter because the heat flow is very large. It is examined that the sample with the intense decomposition can be measured using the CPVT. The samples are a lithium coin battery and a lithium ion battery. In addition, the intensity in decomposition of the lithium coin battery is measured with the differential accelerating rate calorimeter (DARC).

2. Experimental

2.1 Apparatus

The temperature and the pressure was measured with the CPVT and the mini CPVT (MCPVT) simultaneously. They were used to investigate the auto-ignition by oxidation and the intense decomposition. The space capacity of CPVT and MCPVT is about 314 cm³ and 8 cm³.

The measurement precision of the CPVT was examined when the transition temperature of potassium nitrate was measured with the CPVT. The measurement result of potassium nitrate by the CPVT is shown Figure 1. The heating rate was 0.13K·min⁻¹. The measurement value of the transition temperature of potassium nitrate was 128.2°C. The reference value is 127.7°C. The similar result was obtained by the measurement of 3.6K·min⁻¹ of the heating rate. The measurement precision of the CPVT was confirmed to be in ± 2 K including the measurement error of the thermocouple.

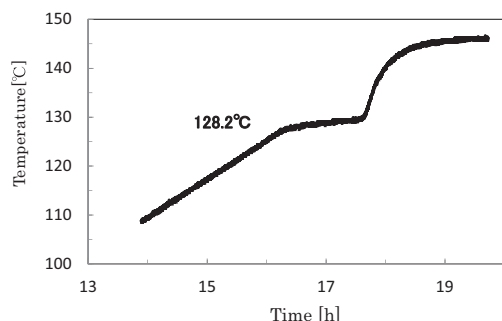


Figure 1 The measurement result of KNO_3 with the CPVT.

The heat detection temperature measured with the C80 was used to investigate the oxidation. The auto-ignition temperature was measured with the SIT. The data of CPVT were compared with those of the C80 and the SIT. The thermal behavior of sample was examined by the thermal activity monitor (TAM).

The DARC were used to investigate the intense decomposition. The DARC can realize the adiabatic measurements on the condition that the phi factor equals to one¹). All of the heat generated from sample was consumed for heating the sample without heating the sample container in the DARC measurement.

2.2 Samples

BDF, linseed oil, squalane and squalene were used as liquid samples which generate the oxidation heat. BDF, linseed oil, and squalene has the double bonds in their intramolecular. Squalane has no double bonds in its intramolecular. RDF, RPF, and subbituminous coal were used as solid samples which generate the oxidation heat. A lithium coin battery (CR1220) and the lithium ion battery (18650) for personal computer were used as samples which cause the intense decomposition.

2.3 Measurement conditions

The measurement conditions were summarized in Table 1. The heating test was conducted by the CPVT, the MCPVT and the C80. The heating rate was set to $0.1\text{K}\cdot\text{min}^{-1}$ in the C80. The isothermal test was conducted by the TAM. The adiabatic test was conducted in the SIT and the DARC test. The measurement period for obtaining the auto-ignition limit temperature (T_{SIT}) was 24 hours in the SIT test. The container of the SIT was made of the glass. The air flow was $2\text{mL}\cdot\text{min}^{-1}$ in the SIT. The adiabatic test of DARC was conducted in the heat-wait-search mode. The measurement started from 70°C . The isothermal step was 5K. The heat rate on the interval of isothermal temperature was $0.5\text{K}\cdot\text{min}^{-1}$. The detection limit was $0.01\text{K}\cdot\text{min}^{-1}$.

2.3.1 Liquid sample

The sample (0.30 g) was soaked in the absorbent cotton (2.3g) in the CPVT. The CPVT test was conducted in various heating rates from $0.065\text{K}\cdot\text{min}^{-1}$ to $0.27\text{K}\cdot\text{min}^{-1}$ (3.9 – $16.0\text{K}\cdot\text{h}^{-1}$).

The sample (0.20 g) was put in glass container without a cap in the C80. The glass container was set in the stainless

container for the C80. The ambient atmosphere was air. The samples were measured in argon excluding linseed oil.

The sample (0.1 g) was soaked in the glass wool (0.08 g) in the SIT. The measurement began when the air was introduced to the sample. The sample (0.5 g) was put in the glass container (1.3 mL) with a screw cap in the TAM. The ambient temperature was 70°C in the liquid samples tests by the TAM.

2.3.2 Solid sample

The sample weight of RDF was 10.0 g in the CPVT. The heating rate was $0.063\text{K}\cdot\text{min}^{-1}$ ($3.8\text{K}\cdot\text{h}^{-1}$). The sample weight of RDF was 1.5 g in the C80. The RDF sample was put into the stainless container in the C80. The sample weight of RDF was 1.4 g in the SIT. The manufacturer of the RDF sample used in the C80 and the CPVT were different from that of the SIT.

The sample weight of RPF was 10.0 g in the CPVT. The heating rate was $0.065\text{K}\cdot\text{min}^{-1}$ ($3.9\text{K}\cdot\text{h}^{-1}$). The sample weight of RPF was 1.5 g in the C80. The RPF sample was put into the stainless container in the C80. The sample weight of RPF was 1.0 g in the SIT. The manufacturer of the RPF sample used in the C80 and the CPVT were different from that of the SIT.

The sample weight of coal was 10.0 g in the CPVT. The heating rate was $0.063\text{K}\cdot\text{min}^{-1}$ ($3.8\text{K}\cdot\text{h}^{-1}$). The sample weight of coal was 1.5 g in the C80. The coal was set in the stainless container. The sample weight of coal was 1.3 g in the SIT. The measurements was conducted under the adiabatic control after water was evaporated perfectly in the sample container of the SIT.

The sample weight of RDF, RPF and coal was 1.0 g in the TAM. The sample was put into the stainless container. The ambient temperature was 50°C in the solid samples tests by the TAM.

2.3.3 Battery sample

The lithium coin battery (CR1220) was measured with the MCPVT and the DARC. The diameter and the thickness of the lithium coin battery was 12.5 mm and 2.0 mm, respectively. The MCPVT was applied to the lithium coin battery because the rise of the pressure and temperature was small in the CPVT. The weight of the lithium coin battery was 0.9 g. The lithium coin battery was heated at the heating rate of $2.4\text{K}\cdot\text{min}^{-1}$ in the MCPVT. The heating rate of battery sample was large compared with liquid sample because the purpose of measurement was to determine the intensity of decomposition. The lithium coin battery with the addition of water (1.0 g) was measured with the MCPVT. The heating rate was $2.2\text{K}\cdot\text{min}^{-1}$.

The lithium coin battery was measured in the heat-wait-research mode of DARC. The lithium coin battery with the addition of water (2.0 g) was measured by the DARC.

The lithium ion battery was measured with the CPVT. The weight of the lithium ion battery (18650) was 44 g. The diameter and the length of the lithium ion battery was 18 mm and 65 mm, respectively. The lithium ion

Table 1 Measurement conditions.

1) Sample weight.

Sample	CPVT [g]	MCPVT [g]	C80 [g]	TAM [g]	SIT [g]	DARC [g]
Liquid samples	0.30	–	0.2	0.5	0.1	–
RDF	10.0	–	1.5	1.5	1.4	–
RPF	10.0	–	1.5	1.5	1.0	–
Coal	10.0	–	1.5	1.5	1.3	–
Coin battery	–	0.9	–	–	–	0.9
Lithium ion battery	44	–	–	–	–	–

2) Temperature control.

Sample	CPVT [Kh ⁻¹]	MCPVT [Kmin ⁻¹]	C80 [Kmin ⁻¹]	TAM [°C]	SIT	DARC
Liquid samples	7.6 (*)(Heating)	–	0.1 (Heating)	70 (Isothermal)	Adiabatic	–
RDF	3.8 (Heating)	–	0.1 (Heating)	50 (Isothermal)	Adiabatic	–
RPF	3.9 (Heating)	–	0.1 (Heating)	50 (Isothermal)	Adiabatic	–
Coal	3.8 (Heating)	–	0.1 (Heating)	50 (Isothermal)	Adiabatic	–
Coin battery	–	2.4 (Heating)	–	–	–	Adiabatic
Lithium ion battery	138 (Heating)	–	–	–	–	–

* : Heating rate when Ta was obtained.

3) Sample conditions.

Sample	CPVT	MCPVT	C80	TAM	SIT	DARC
Liquid samples	Soaked in cotton wool	–	Glass container without cap	Glass container with cap	Soaked in silica wool	–
Solid samples	Put container for apparatus	–	Put in container for apparatus	Put in container for apparatus	Put in container for apparatus	–
Coin battery	–	Put in apparatus	–	–	–	–
Lithium ion battery	Put in apparatus	–	–	–	–	Put in container for apparatus

4) Other conditions.

Condition	CPVT	MCPVT	C80	TAM	SIT	DARC
Container for apparatus	No containers	No containers	Stainless container	Stainless container	Glass container	Stainless container
Temperature range for measurement [°C]	25–360	25–250	25–200	50,70	50–130	70–350
Ambient atmosphere	Air	Air	Air, argon	Air	Air flow	Air
Water addition test	–	Done (1.0 [g])	–	–	–	Done (2.0 [g])

battery was heated at heating rate of 2.3K·min⁻¹ (138K·hr⁻¹) in the CPVT. The lithium ion battery could not be measured with the DARC because it could not be put in the sample container of DARC

3. Results and discussion

The measurement results of liquid and solid sample are summarized in Table 2. The heat detection temperature (Ta) is the temperature at which the obvious temperature increase begins in the base-line of the time-temperature curve of the liquid sample. The Ta could not be detected with the CPVT in the solid samples. The pressure detection temperature (Tb) is the temperature at which the obvious pressure increase begins in the base-line of the temperature-pressure curve of the solid sample. The unit of pressure is the gauge pressure in all tests.

3.1 Liquid sample

The Ta values obtained with the CPVT were about 20-

Table 2 Results of heat detection temperature and auto-ignition temperature.

Sample	CPVT	C80	SIT(24h)
	Ta or Tb [°C]	Ta [°C]	TsIT [°C]
BDF	88	66	80
Linseed oil	109	72	70
Squalane	149	112	130
Squalene	113	75	95
RDF	175	128	140
RPF	188	136	127
Coal	115	37	95

1) The heat detection temperature (Ta) is the temperature at which the obvious temperature rise begins.

2) The pressure detection temperature (Tb) is the temperature at which the obvious pressure increase begins.

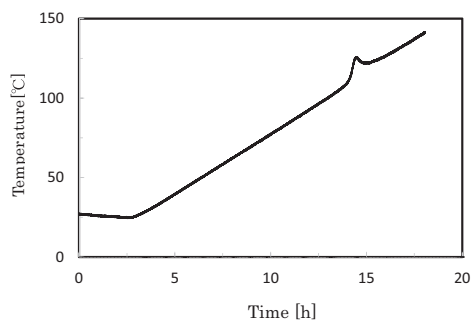


Figure 2 The temperature curve of linseed oil measured with the CPVT.

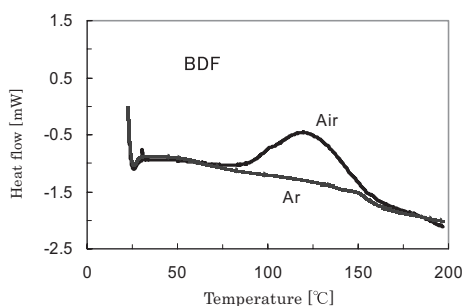


Figure 4 Heat flow curve of BDF measured with the C80.

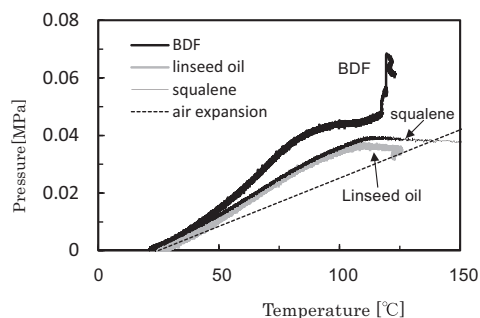


Figure 3 The pressure-temperature curve measured with the CPVT.

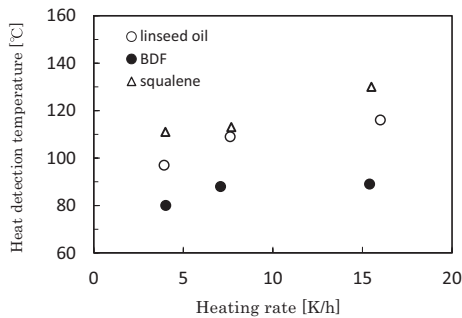


Figure 5 The relationship between heat rate and heat detection temperature (T_a) measured with the CPVT.

40K higher than the T_a values measured with the C80 in the liquid sample. The heating rate of CPVT was $0.13\text{K}\cdot\text{min}^{-1}$ ($7.6\text{K}\cdot\text{h}^{-1}$). The onset of the decomposition was recognized as the onset of temperature rise in the liquid samples. The T_a values measured with the C80 were about 10-20K higher than the T_{SIT} values measured with the SIT. T_a measured with the C80 and the T_{SIT} obtained with the SIT had the correlation with T_a measured with the CPVT. The T_a of squalene was higher than that of squalane in Table 2. Squalane was not oxidized easily than squalene because it has no double bonds in intramolecular. This hazard of oxidation was consistent with T_a measured with the CPVT.

The time-temperature curve of linseed oil measured with the CPVT is shown in Figure 2. The heating rate was $0.13\text{K}\cdot\text{min}^{-1}$ ($7.6\text{K}\cdot\text{h}^{-1}$). It was demonstrated that the CPVT could detect the oxidation heat because the temperature peak was observed. The similar temperature peaks in the time-temperature curve were in the other liquid samples.

The temperature-pressure curve of linseed oil, squalene and BDF measured with the CPVT is shown in Figure 3. The dot line indicates the pressure rise by the expansion of air for the temperature rise. The pressure rise by the evaporation of sample was measured in both of samples. The pressure rise stopped and became a plateau. This reason was because oxygen absorbed in the sample soaked in the absorbent cotton². There was little pressure rise in the linseed oil and the squalene. They did not generate the decomposition gas so much. BDF generated decomposition gas more than the linseed oil and the squalene.

The heat flow curve of BDF measured with the C80 is shown in Figure 4 in air and argon (Ar) atmosphere. The heat flow peak was not observed in argon. The same results were obtained regarding to squalane and

squalene³. This reason was that BDF, squalane, and squalene generated the oxidation heat. The oxidation heats of the BDF, the linseed oil and squalene obtained with the C80 were $125.1\text{J}\cdot\text{g}^{-1}$, $96.6\text{J}\cdot\text{g}^{-1}$, and $103.4\text{J}\cdot\text{g}^{-1}$, respectively. These values indicated that the enough possibility that these sample cause fire because these values were much higher than the heat of the sample that caused a fire by fermentation (about $14\text{J}\cdot\text{g}^{-1}$)⁴. This reference value was measured with the TAM at 50°C . The limit value of heat is about more than $10\text{J}\cdot\text{g}^{-1}$ in the range from the room temperature to 100°C in the measurement of the C80 and the TAM in

our recent research⁵.

The relationship between the heating rate and T_a obtained with the CPVT is shown in Figure 5. The T_a values were almost constant against heating rate in the BDF samples. The heating rate was not affected by the increase of T_a in BDF. The T_a values increased with the increase of heating rate in the linseed oil and squalene samples. The heating rate was affected by the increase of T_a in the linseed oil and squalene. This showed that the decomposition mechanism was different in both of samples.

The heat flow curves of BDF and the linseed oil measured with the TAM at 70°C were shown in Figures 6 and 7, respectively. The oxidation heats of the BDF and the linseed oil obtained with the TAM were $14.7\text{J}\cdot\text{g}^{-1}$ and $76.2\text{J}\cdot\text{g}^{-1}$ at 70°C when the measurement period was 72 hours. The heat flow increased from the onset of measurement and the heat flow had a peak and decreased beyond a peak in the BDF. The decrease rate of heat flow decreased around eight hours from the beginning of measurement. The heat flow curve of BDF showed two step reactions. It was reported that the first heat flow peak of BDF showed the auto-catalytic style⁶. The heat flow increased from the onset of measurement and the heat flow had a peak and decreased beyond a peak in the linseed oil. The similar result was obtained from the squalene and the squalane sample. The heat flow curve of the linseed oil had one step reaction. The difference in the reaction mechanism in their decompositions was reflected on the behavior of the pressure rise when the sample was heated.

3.2 Solid sample

The T_b values obtained with the CPVT were about 20-60K higher than T_{SIT} values. The onset of the

decomposition was recognized as the onset of temperature rise. The onset of the decomposition was recognized as the onset of pressure rise in the solid samples.

The time-pressure curve of RDF measured with the CPVT is shown in Figure 8. The pressure rise was obtained with the CPVT when RDF was heated. The temperature peak could not be detected from the time vs. temperature curve of RDF. The T_b of RDF was obtained from the temperature when the obvious pressure rise began in the base-line on temperature vs. pressure curve. The onset of the decomposition was

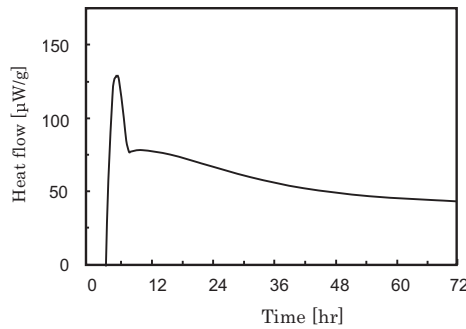


Figure 6 Heat flow curve of BDF measured with the TAM at 70°C.

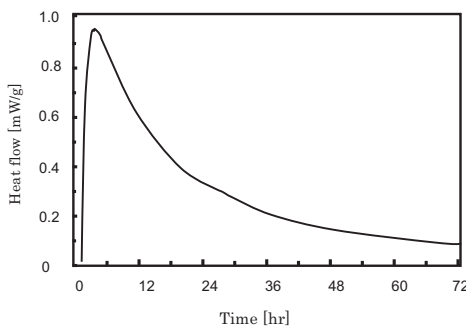


Figure 7 Heat flow curve of linseed oil measured with the TAM at 70°C.

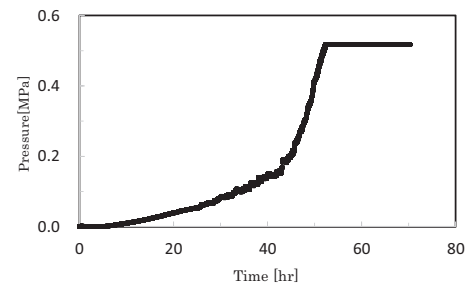


Figure 8 Pressure curve of RDF measured with the CPVT.

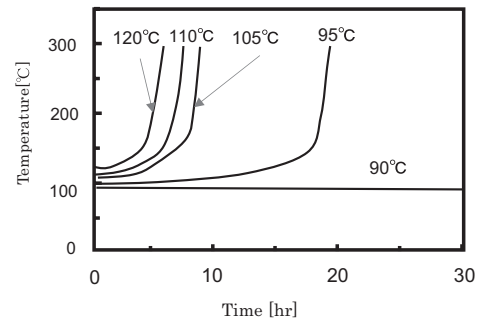


Figure 9 Time vs. sample temperature curves of coal measured with the SIT. The numbers indicate the ambient temperature.

recognized as the onset of pressure rise. RDF generated much decomposition gas when the sample temperature was beyond 175°C⁶⁾. The C80 could measure the small heat generation which was detected from 53°C and the large heat generation which was detected from 128°C. The large heat generation led to the combustion of RDF. The CPVT could not detect the small peak, but detect the large peak. The T_b of RDF measured with the CPVT was derived from the oxidation corresponded to the large heat generation in the C80.

RPF was measured with the CPVT. The C80 could measure the large heat generation which was detected from 136°C. The large heat generation led to the combustion of RPF. The gas generation was observed at about 120°C by the CPVT because the small rise of pressure was detected. The large pressure rise was measured at about 188°C.

The T_b value of the coal measured with the CPVT was 115°C. The T_a value obtained with the C80 was 37°C because C80 could detect the small heat generation in the oxidation of coal. The oxidation heat of the coal obtained with the C80 was 14.7J·g⁻¹. The oxidation heat of the coal by the TAM was 22.7J·g⁻¹ at 50°C. The coal had the oxidation heat enough to bring the auto-ignition. The time vs. sample temperature of coal curves measured with the SIT are shown in Figure 9. The numbers in Figure 9 are the ambient temperature. T_{SIT} was 95°C. The T_{SIT} value was close to T_a measured with the CPVT. The large heat generation in the oxidation of coal was measured with both of the CPVT and the SIT. The small heat generation from about 40°C could not be measured with the CPVT and the SIT.

3.3 Battery sample

The pressure rise was not detected without the addition of water in the MCPVT of lithium coin battery excluding

the pressure rise of the expansion of air for the temperature rise. The pressure rise by the decomposition began from about 200°C when the water (1.0 g) was added to the sample. The pressure rise of about 0.77MPa was detected at 230°C. The pressure of water vapor was about 0.30MPa at 230°C when only water was measured with the MCPVT.

The heat rate vs. temperature curve of the lithium coin battery obtained with the DARC is shown in Figure 10. The temperature vibration to about 150°C was due to the temperature control in the heat-wait-search mode. The heat generation and pressure rise of the lithium coin battery could be measured with DARC clearly compared with the CPVT and the MCPVT. The measurement of the DARC was conducted to 310°C. The heat onset temperature was 155°C without the water addition. The maximum heat rate was 81K·min⁻¹. The maximum pressure and the maximum pressure rise rate were 0.395 MPa and 0.197MPa/min without the water addition. When water (2.0 g) was added, heat onset temperature decreased to 130-140°C. The maximum pressure and the maximum pressure rise rate increased to 0.663MPa and 0.364MPa·min⁻¹. The hazard of decomposition increased when water was added. It was thought that the reaction of the metallic lithium and water had influenced on the increase of pressure hazard. The lithium ion battery was examined by the CPVT. Only the CPVT can measure its hazard because the sample is large and the decomposition of sample is very intense.

The results of time vs. temperature and pressure of the lithium ion battery measured with the CPVT are shown in Figure 11. The charging rate was near the full charge. The lithium ion battery caused the intense decomposition when it was heated. The bursting disc operated at about 157°C when 4,350 seconds was elapsed. The intense decomposition occurred beyond about 190°C. In contrast,

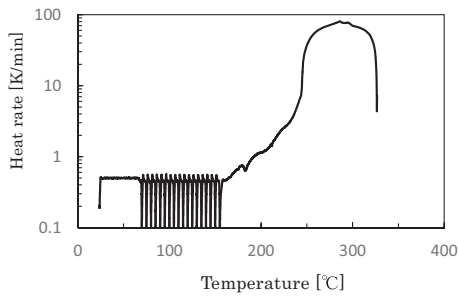


Figure 10 Temperature vs. heat rate of lithium coin battery measured with the DARC.

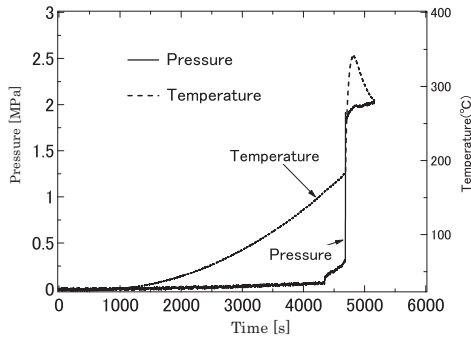


Figure 11 Time vs. temperature and pressure curves of lithium ion battery measured with the CPVT.

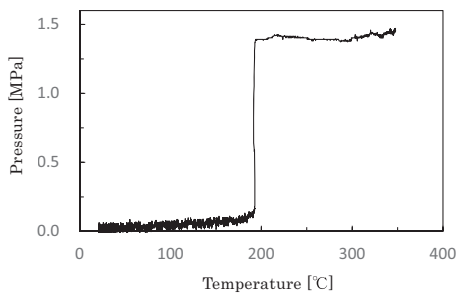


Figure 12 Temperature vs. pressure curve of re-heated lithium ion battery measured with the CPVT.

when the charging rate was near 0%, the intense decomposition did not occur.

A positive electrode of the lithium-ion battery is made of metal oxides including lithium (LiCoO_2). A negative electrode pole is made of graphite. The organic solution including lithium salt is used as the electrolytic solution. A positive electrode changes to cobalt oxide (CoO_2) in the electrical charge state. A negative electrode changes to graphite including metal lithium in the electrical charge state. The positive electrode changes to LiCoO_2 in the electrical discharge state. The negative electrode changes to graphite in the electrical discharge state. The electrical charge and discharge were conducted by the lithium ion moving between the positive electrode and the negative electrode.

The cause of the intense decomposition of the lithium ion battery was studied by the following experiment. The heating of the battery was stopped when the bursting disc operated. At the time, the intense decomposition had not occurred yet. The battery which operated the bursting disc was cooled to the room temperature. The battery was taken out of the CPVT. The voltage of this battery was nearly zero volt. Next, the battery which bursting

operated was heated again.

If the re-heated battery made the intense decomposition, it was supported that the intense decomposition of the battery was caused by the reactive substance generated in the battery. In the other hand, if the re-heated battery did not make the intense decomposition, it was supported the intense decomposition of the battery was caused by the electrical energy such as the electrical short.

The result of temperature vs. pressure of the re-heated battery measured with the CPVT is shown in Figure 12. The intense decomposition was observed beyond about 190°C. This intense decomposition was corresponded to the intense peak after the bursting disc operating in Figure 11. This indicated that the reactive substance was generated in the lithium battery. There was the possibility that the reactive substance was CoO_2 of the spinel structure with the cubic system⁸). CoO_2 was made by the elimination of lithium from LiCoO_2 by the charge. The CoO_2 of the layer structure with the hexagonal crystal system was changed to CoO_2 of the spinel structure with the cubic system by heat.

4. Conclusions

A closed pressure vessel test (CPVT) was developed in order to measure the temperature and the pressure in the decomposition of sample.

The rise of the temperature could be measured in the oxidation of liquid sample. The temperature on the onset of the pressure rise could be measured in the oxidation of solid sample. The decomposition behavior of lithium ion battery was measured with the CPVT. The lithium ion battery brought the intense decomposition. The intense decomposition of the lithium ion battery was suggested to be caused by the reactive substance generated during heating.

Acknowledgment

The part of the battery of this research was supported by the Environment Research and Technology Development Fund (3K113011) of the Ministry of the Environment, Japan.

References

- 1) Y. Iwata, *Sci. Tech. Energetic Materials*, 74, 160–164 (2013) 15–20 (2006).
- 2) Y. Iwata, the Proc. Forty-Seventh Meeting on Safety Engineering, 109–110 (2014) (in Japanese).
- 3) Y. Iwata, Proc. Forty-Sixth Meeting on Safety Engineering, 41–42 (2013) (in Japanese).
- 4) Xin-Rui Li, H. Koseki, and M. Momota, *Journal of Hazardous Materials*, A135, 15–20 (2006).
- 5) Yusaku Iwata, *Journal of Japan Society for Safety Engineering*, 53, 410–417 (2014) (in Japanese).
- 6) Y. Iwata, Proc. Meeting on Japan Association for Fire Science and Engineering, 304–305 (2012) (in Japanese).
- 7) Y. Iwata, Proc. Forty-Fourth Symposium on Safety Engineering, 360–361, (2014) (in Japanese).
- 8) S. Kitano, Y. Uebou, H. Wada, T. Aoki, and T. Murata, *GS Yuasa Technical Report*, Vol.2(2), 18–24 (2005) (in Japanese).